Colloid Polym Sci (2007) 285:1361–1367
DOI 10.1007/s00396-007-1694-9

ORIGINAL CONTRIBUTION

Microstructure and structural transition in palm-kernel oil microemulsion using 1.5-order differential electroanalysis

Chunsheng Mo · Xiaoge Li

Received: 6 February 2007 / Accepted: 5 May 2007 / Published online: 2 June 2007

Abstract The microemulsification in palm-kernel oil/cetyltrimethylammonium bromide/*iso*-pentanol/water system is investigated. The effect of iso-pentanol concentration in microemulsions on the size of single-phase microemulsion region is also discussed. It is found that the maximum microemulsion domain is obtained when *iso*-pentanol-to-cetyltrimethylammonium bromide mass ratio is 1.75. The diffusion coefficients of electroactive probe (ferrocene) in microemulsion microenvironment are measured by 1.5-order differential electroanalysis. The microstructure and structural transition from water-in-oil to oil-in-water microemulsions through a bicontinuous structure is examined. The results are found to be in agreement with that of conductivity measurements.

Keywords Cetyltrimethylammonium bromide · Palm-kernel oil · Microemulsion · 1.5-order differential electroanalysis · Conductivity · Diffusion coefficient

Introduction

Electrochemical techniques, such as polarography, rotation disk voltammetry, chronocoulometry, and cyclic voltammetry as the popular tools for colloid and surface chemists, have been successfully applied in the study of physicochemical properties of aqueous surfactant solutions [1–10]. In addition to being less sophisticated and generally less time-consuming, electrochemical measurements are useful for characterizing organized surfactant solutions. However, the limitation of these methods lies in the fact that the concentration of an electroactive probe and/of the supporting electrolyte in solutions should be moderately high because the internal resistance of solution is high in the presence of surfactant and hydrocarbon. Adding sufficient electroactive probe and the supporting electrolyte into a surfactant solution must cause some changes in properties of the dispersion, which makes the parameters obtained from electrochemical measurements not true to the original in a sense. To overcome these shortcomings, we attempt to use a novel technique—the differential electroanalysis—for characterizing surfactant solutions. The advantage of this approach over general voltammetric methods lies in its high sensitivity and resolving power to the change of current produced on the working electrode when a chemical reaction occurs. In this work, cetyltrimethylammonium bromide/palm-kernel oil/*iso*-pentanol/water system was examined by 1.5-order differential electroanalysis using an electroactive probe ferrocene to determine the diffusion coefficients of microemulsion droplets and to detect microstructure inversion in the microemulsion region. We chose this system, as its phase behavior is still unknown up to now; in particular, microemulsification of vegetable oils is a field of much current interest [11–15].

C. Mo (✉) · X. Li
Chemistry Science and Technology School,
Zhanjiang Normal University,
Zhanjiang 524048 Guangdong Province,
People's Republic of China
e-mail: surfac56@yahoo.com.cn

Experimental section

Chemicals and reagents

The surfactant cetyltrimethylammonium bromide ($C_{16}H_{33}N^{+}(CH_3)_3Br^{-}$, abbreviated as CTAB) is obtained from the Nanjing Robiot (China) and is washed repeatedly with ether and then recrystallized three times with an acetone +

methanol + water [90:5:5(*v*/*v*)] mixture and dried in vacuo for 24 h at room temperature. The purity is checked by the absence of a minimum in the plot of surface tension vs concentration. The edible refined palm-kernel oil is a product of Buer Industries (China). The cosurfactant is *iso*-pentanol (A.R. grade). Ferrocene (Fc) is used as the electroactive probe. Doubly distilled and deionized water is used.

Apparatus and procedure

The phase behavior of palm-kernel oil + cetyltrimethylammonium bromide + *iso*-pentanol + water four-component system is represented in a pseudo-ternary phase diagram, in which water is one component, another one is palm-kernel oil, and the third component is an emulsifier (EM), which is a mixture of CTAB + *iso*-pentanol. The ternary phase diagram is constructed adopting a simple titration technique: an emulsifier (EM) in which the cosurfactant-to-surfactant mass ratio, $k_m = W(\text{alcohol})/W(\text{CTAB})$, is fixed, is first prepared by combining the required mass of the cosurfactant and surfactant, then an appropriate quantity of palm-kernel oil is introduced into the emulsifier. In this mixture, the initial oil content, R, is fixed but may be changed. Water is the titration component. Adding the water to a mixture of the oil + emulsifier, a water-in-oil (*W*/*O*) microemulsion is obtained firstly. The phase boundary is noted by observing the transition from turbidity to transparency or from transparency to turbidity. By repeating this experimental procedure for other values of R (for example, R=0.05, 0.1, 0.15, 0.2,..., 0.95), the boundaries of the microemulsion domain corresponding to the chosen value of k_m are determined. The content of each component in solutions is derived from precise mass measurements.

The 1.5-order differential electroanalysis measurements are performed using an electrochemical analyzer model XJP-821(c)(Jiangsu Electrochemical Instruments, China) equipped with a 3036 X–Y recorder(Sichuan Instruments Factory). A glassy carbon working electrode, a saturated calomel reference electrode (SCE; all experimental potentials are referred to this electrode), and a platinum counter electrode are used. The working electrode area is determined using cyclic voltammetry experiments on a reversible system (4 mM $K_4Fe(CN)_6$ in 1 M KCl). By use of the diffusion coefficient $D=6.3\times10^{-10}$ m^2 s^{-1} [16], the electrode area is $A=3.3\times10^{-6}$ m^2. The potential is scanned between 0.0 and 0.8 V, and the sweep rate range used is 20 to 100 mV s^{-1} in this work.

The microemulsion conductivity, κ, is measured by means of a DDS-11A conductivity meter (Rex Instruments Factory, China) equipped with a DJS-1 or DJS-10 platinum conductance electrode coated with platinum black.

All the titration experiments and electrochemistry measurements are performed in an airconditioned room in which the temperature is kept at 28±1 °C.

Results and discussions

Microemulsification of palm-kernel oil

Figure 1 shows the phase behavior of a palm-kernel oil + CTAB + *iso*-pentanol + H_2O system for various k_m values at 28 °C. The region marked "μE" is the one-phase microemulsion. Within "two-phase" region, a microemulsion phase can exist in equilibrium with an excess oil phase when the initial oil content R is high. However, a microemulsion phase and turbid macroemulsion are in equilibrium at medium initial oil content. It is evident from Fig. 1 that there is a significant effect of the *iso*-pentanol-to-CTAB mass ratio, k_m, on the area of single-phase microemulsion region in palm-kernel oil/CTAB/*iso*-pentanol/H_2O system. A relatively larger single-phase microemulsion region exists when the value of k_m lies in the range of 1.5–1.75; there is an obvious decrease in the area of microemulsion region when the value of the k_m deviates from this range. In fact, the effect of values of k_m on the area of microemulsion region corresponds to the effect of alcohol concentration at given conditions. It is generally known [17–19] that alcohol is essential in promoting interfacial fluidity for the formation of microemulsions. The addition of alcohol can cause the alcohol partitioning at the interface. At moderately low alcohol concentrations, this can increase the total interfacial area for solubilization and consequently increase the area of microemulsion region. However, at sufficiently high alcohol concentrations, the fluidity of the interface increases to the extent at which attractive interdroplet interaction starts dominating the system, and hence the solubilization decreases. Therefore, there is an optimal value of k_m at which the area of single-phase microemulsion region reaches the maximum for any microemulsion system. This optimal value of k_m was 1.75 in the investigated system for *iso*-pentanol cosurfactant.

The diffusion coefficient of ferrocene and microstructure of the microemulsion

The differential electroanalytical method was first introduced in 1975 by Goto and Ishii [20] based on the integral electroanalysis method. The semidifferential electroanalysis measures the semidifferential of current against the electrode potential. In the case of the reversible electrode reaction, the following relationship between the electrode potential, E, and the semidifferential of current, $e(t)$, applies for a planar electrode and a ramp signal:

$$e(t) = \frac{d^{1/2}}{dt^{1/2}} i(t) = \left(n^2F^2A\upsilon D^{1/2}c/4RT\right) \times \left[\sec h^2\left[(nF/2RT)\left(E - E_{1/2}\right)\right]\right] \quad (1)$$

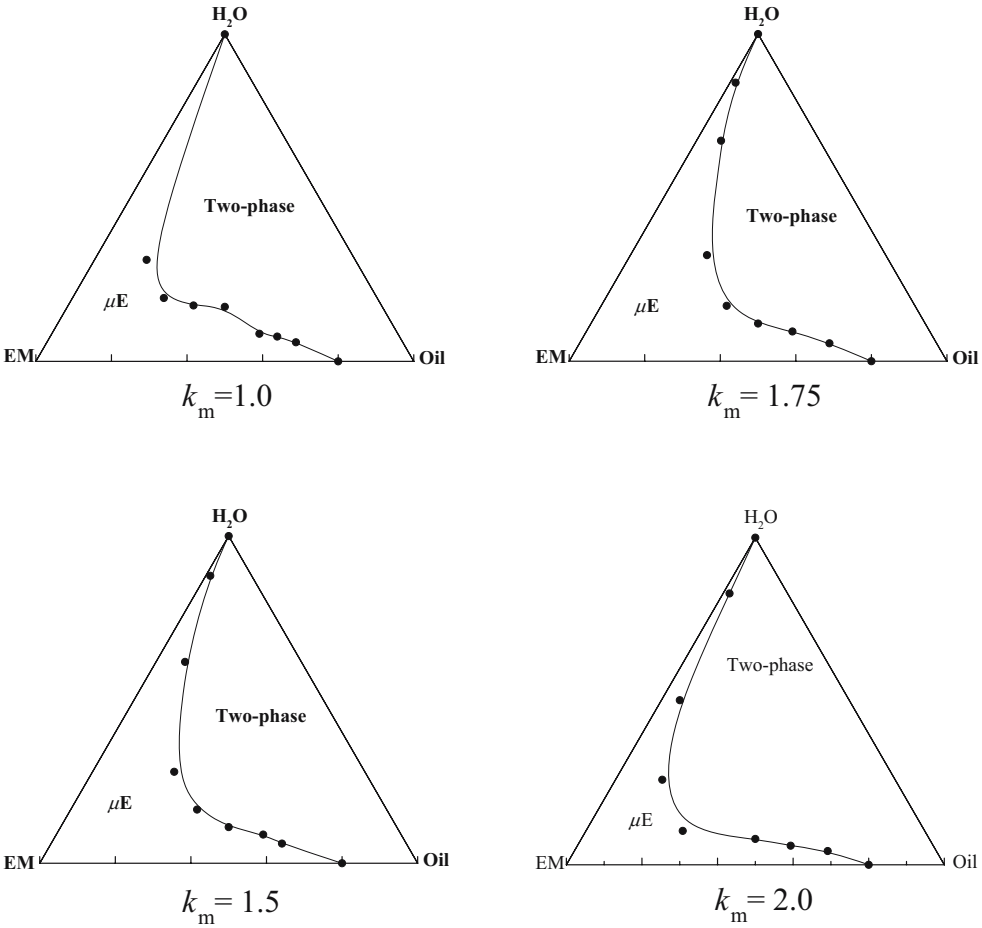

Fig. 1 Phase diagrams of the pseudoternary of palm-kernel oil/CTAB/*iso*-pentanol/water system for various k_m values at 28 °C. Effects of the alcohol content on the formation of microemulsion

where i is the peak current in the linear sweep voltammetry, $E_{1/2}$ is the half-wave potential, n is the number of electrons involved in oxidation or reduction, F is the Faraday constant, A is the area of the electrode, c is the concentration of electroactive probe, R is the gas constant, T is the absolute temperature, D is the diffusion coefficient of the electroactive probe, and υ is the scan rate.

Differentiating the semidifferential of current, $e(t)$, with respect to time, t, we obtain e', the 1.5-order differential of current, as a function of the electrode potential, E [21]:

$$\begin{aligned} e'(t) &= \frac{d^{3/2}}{dt^{3/2}} i(t) \\ &= \left(n^3 F^3 A\, \upsilon^2 D^{1/2} / 4R^2 T^2\right) \sec h^2(x) \tanh(x) \end{aligned} \tag{2}$$

where $x=(nF/2RT)(E-E_{1/2})$. A plot of the function $\text{sech}^2(x)\tanh(x)$ against x is noted in Fig. 2. The curve is comprised of a maximum peak (the peak value is 0.3849 when $x=0.66$) and a minimum peak (the peak value is -0.3849 when $x=-0.66$); they are exact inversion symmetry about the half-wave potential in the case of the reversible electrode reaction. The positive and negative peak potential E_{pp}, E_{np}, therefore, can be easy obtained from $x = (nF/2RT)\left(E - E_{1/2}\right) = \pm 0.66$:

$$E_{pp} = E_{1/2} + 1.32(RT/nF) \tag{3}$$

$$E_{np} = E_{1/2} - 1.32(RT/nF) \tag{4}$$

Eq. 5 indicates the peak height e'_p (with $\text{sech}^2(x)\tanh(x) = 2\times 0.3849$),

$$e'_p = \left(0.77 n^3 F^3 A\, \upsilon^2 D^{1/2} c / 4R^2 T^2\right) \tag{5}$$

Note that Eqs. 3, 4, and 5 are derived from a mode, which assumes linear diffusion to a planar electrode; concentration variations can only occur perpendicular to the electrode surface. It follows from Eqs. 3 and 4 that the peak potentials E are independent of the scan rate and the concentration c, which can be used to carry a qualitative analysis, and the peak height e'_p is directly proportional to the concentration c, the area of the electrode A, and the scan rate υ^2, which is the theoretical basis of the quantitative analysis. A plot of e'_p

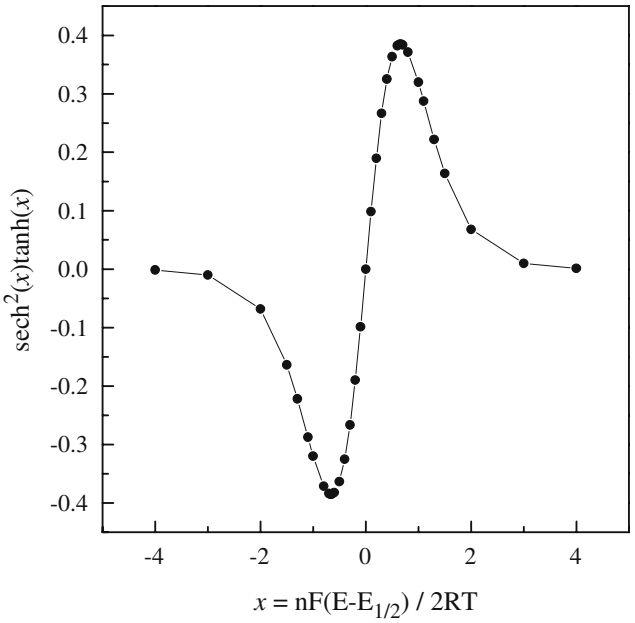

Fig. 2 Shape of sech^2(x)tanh(x) against x curve

against υ^2 should give a straight line; the diffusion coefficient D can be calculated from the slope of this line.

To examine the microstructure of microemulsion droplets, we use an oil-soluble Fc as the electroactive probe in 1.5-order differential electroanalysis. A small amount of the electroactive probe (Fc, 0.0024 g) is first dissolved in 0.5000 g of palm-kernel oil; then 2.7000 g of iso-pentanol and 1.8000 g of CTAB are added in turn. This mixture is titrated with water. We find that a continuous stable single-phase microemulsion can always be observed over the range of water content from >0 to ≤85.3 wt%. The 1.5-order differential electroanalysis is carried out in this microemulsion region at different water contents. Figure 3 illustrates typical e'_p against E curves for Fc in water-in-oil (a) and oil-in-water (b) microemulsions. It is clear from Fig. 3 that the electrochemical response of Fc in microemulsion medium is highly sensitive at each scan rate, the peak potentials are only slightly dependent of the scan rate. A comparison of (a) with (b) in Fig. 3 shows that the half-wave potential $E_{1/2}$ shifts from 0.37 V at water content of microemulsion 1.0 g to 0.16 V at water content 10.0 g; this may be related to the change of microenvironment of microemulsions. The observed decrease of the half-wave potential $E_{1/2}$ of Fc with increasing water content in the microemulsion solutions is in agreement with the half-wave potential measurements of Ohsawa and Aoyagui [22]. They found that the reversible half-wave potential of the ferricinium/ferrocene redox couple in aqueous 0.2 M Li_2SO_4 was 0.165±0.05 V vs SCE, and the reversible half-wave potentials of this couple in cationic micellar solutions of alkyltrimethylammonium bromide was in the range of 0.210–0.252 V, depending on the type and concentration of surfactant used. The differential voltammograms in Fig. 3 and the linear dependency of e'_p on υ^2 in Fig. 4 clearly indicate that the electron transport properties of Fc^+/Fc electrode reaction in the microemulsion medium are diffusion-controlled.

Figure 5 demonstrates the diffusion coefficients of the probe D as a function of the water content of microemulsions. As shown in Fig. 5, D decreases with increasing water content over the entire single-phase microemulsion region. At water contents lower than 29.6%, this decrease is gradual; an abrupt decrease in the diffusion coefficient is observed at water contents in the range from 29.6 to 58.4%, and a gently sloping curve is observed at water contents above 58.4%. Ferrocene is expected to probe the oil environment because of its limited water solubility. At low water contents, a water-in-oil microemulsion is formed, and the oil is the medium. In this case, D is found to be relatively high. The diffusion coefficient of ferrocene at a water content lower than 29.6% changes slowly. This fact indicates that the microenvironment of microemulsions remains unchanged. A similar behavior is observed in this microemulsion at high water contents (above 58.4%). In the latter case, the oil microdroplets are dispersed in a water medium, and the D of ferrocene can be considered as that of oil-in-water microemulsion droplets. However, a dramatic change in the diffusion coefficient of ferrocene is observed at water contents in the range 29.6 to 58.4%. This fact is indicative of a change in the microenvironment of microemulsions. In other words, neither water-in-oil nor oil-in-water microemulsions exist in this region. We can suggest that a bicontinuous microstructure is formed [23]. The bicontinuous microemulsion is a microstructure in which both aqueous and oil solutions are local continuous phases; the microemulsion as a whole may be considered as a coarse network composed from water tubes in a continuous oil medium or oil tubes in a water matrix. The sharp reduction of the diffusion coefficient of Fc in bicontinuous region results from the separation effect of water tubes; this separation effect decreases the fluidity of Fc in oil continuous phase. With further addition of water, the number of water tube increases, which may lead to the formation of oil discontinuous region. The process will progress in the microemulsion solutions when the water content is raised further, and finally, the microemulsion can undergo a phase inversion from bicontinuous type to water continuous constructure at high water contents. It should be pointed out that microemulsions are systems consisting of water, oil, and amphiphile(s) that constitute a single optically isotropic and thermodynamically stable liquid solution. Although microemulsion may change its type from water-in-oil to oil-in-water through a bicontinuous structure under certain experimental conditions, microemulsions are either transparent or semitransparent to

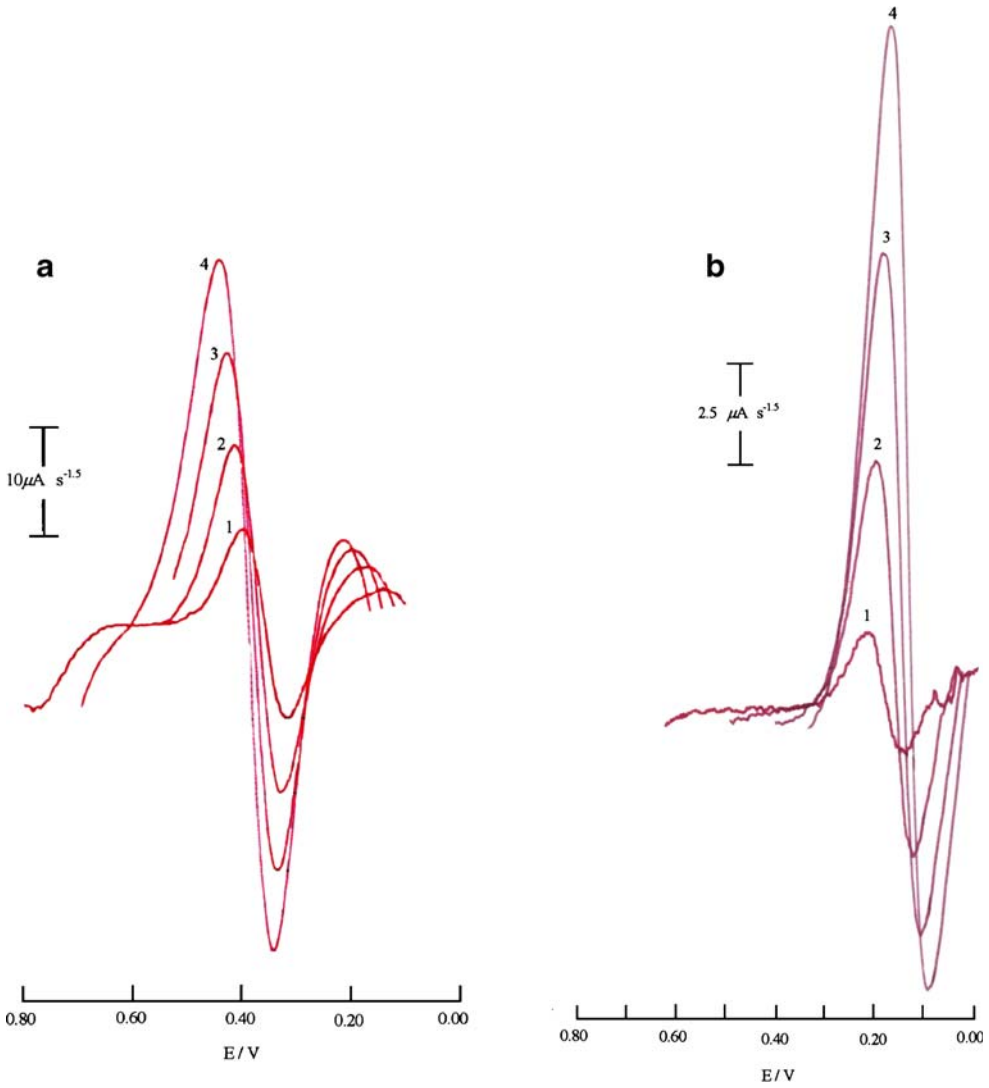

Fig. 3 The electrochemical behavior of ferrocene in **a** *W/O*, **b** *O/W* microemulsions at 28 °C, respectively. Sample solutions: **a** 0.0024 g of Fc, 1.8000 g of CTAB, 0.5000 g of palm-kernel oil, 2.7000 g of *iso*-pentanol, and 1.0000 g H_2O, **b** 0.0024 g of Fc, 1.8000 g of CTAB, 0.5000 g of palm-kernel oil, 2.7000 g of *iso*-pentanol and 10.0000 g H_2O. Scan rates: **a** 40, 60, 80, and 100 mV s^{-1}, **b** 20, 40, 60, and 80 mV s^{-1}

visible light because the size of the dispersed particles in this system lies in the range of 10–250 nm. As already mentioned, we perform a 1.5-order differential electroanalysis in a single-phase microemulsion region over the range of water content from >0 to ≤85.3 wt%; this single-phase channel is nicely suited for the study of the inversion process of a water-in-oil to an oil-in-water microemulsion through a bicontinuous structure. We find that the microstructural transition happens completely continuously without any phase separation.

Conductivity and microstructure of the microemulsion

The determination of the microstructure of microemulsions using conductivity data is based on the percolation theory [24]. For conductor–insulator composite materials, the effective conductivity, κ, is zero as long as the conductor volume fraction Φ is smaller than a critical value Φ_c, called the percolation threshold, because there is no connection between the disperse conducting particles. Suddenly, nonzero values occur when Φ becomes slightly greater than Φ_c and then increases with Φ, owing to the formation of an "infinite cluster" of conducting particles. In the vicinity of Φ_c, the dependency of κ on Φ can be demonstrated in the case of three-dimensional systems by the following power law [25]

$$\kappa(\Phi) \propto (\Phi_c - \Phi)^{8/5} \tag{6}$$

As Φ further increases, the power law is no longer valid, and the conductivity increases according to the following linear law:

$$\kappa(\Phi) \propto (\Phi - \Phi_c) \tag{7}$$

We have also measured the conductivity of several microemulsion samples. Figure 6 shows a typical experimental result. The conductivity κ plotted against water content exhibits features characteristic of percolate conduction. At

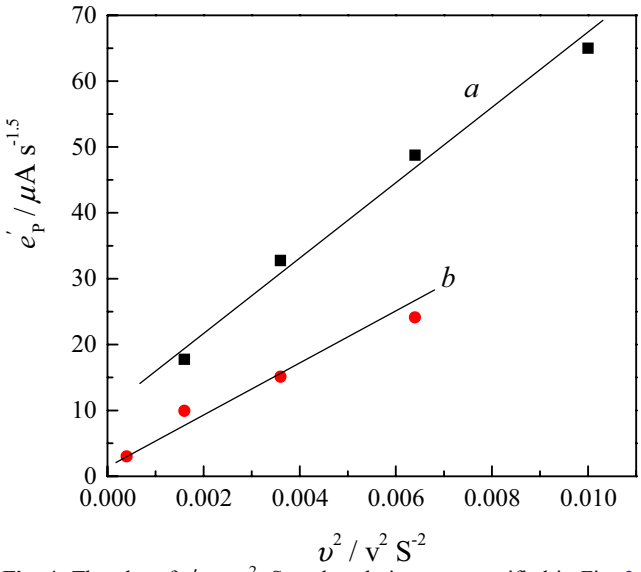

Fig. 4 The plot of e'_p vs υ^2. Sample solutions are specified in Fig. 3

$\Phi<\Phi_b$, the conductivity of microemulsions, κ, linearly and steeply increases up to $\kappa=\kappa_b$, which indicates the formation of an "infinite cluster" of the water-in-oil microdroplets. At high water contents, for example, at $\Phi>\Phi_m$, the value of κ, after arriving at the maximum value κ_m, decreases with increasing water content. This obvious decrease in the conductivity κ results from dilution with the added water, which decreases the concentration of the dispersion phase. Evidently, an oil-in-water microemulsion is formed in this region of high water content. However, in the region of moderate water content at $\Phi_b < \Phi < \Phi_m$, the conductivity curve exhibits an abnormal behavior, κ nonlinearly increases up to a maximum. This feature of conductivity curve is often

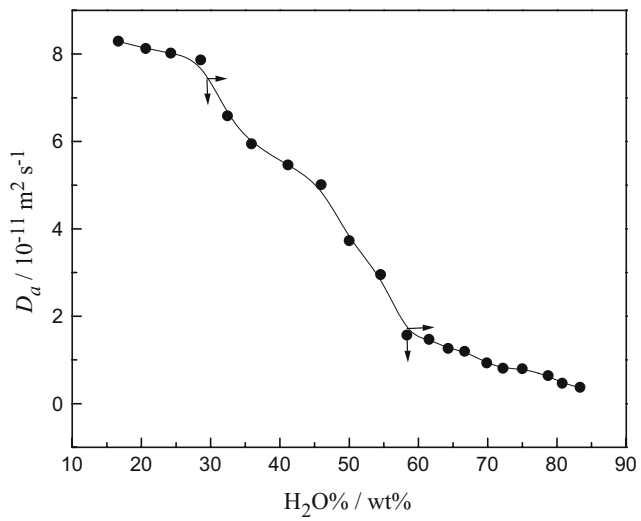

Fig. 5 The diffusion coefficient of ferrocene as a function of water content in a single-phase microemulsion region. The initial composition of system is: 0.0024 g Fc + 1.8000 g CTAB + 0.5000 g palm-kernel oil + 2.7000 g *iso*-pentanol

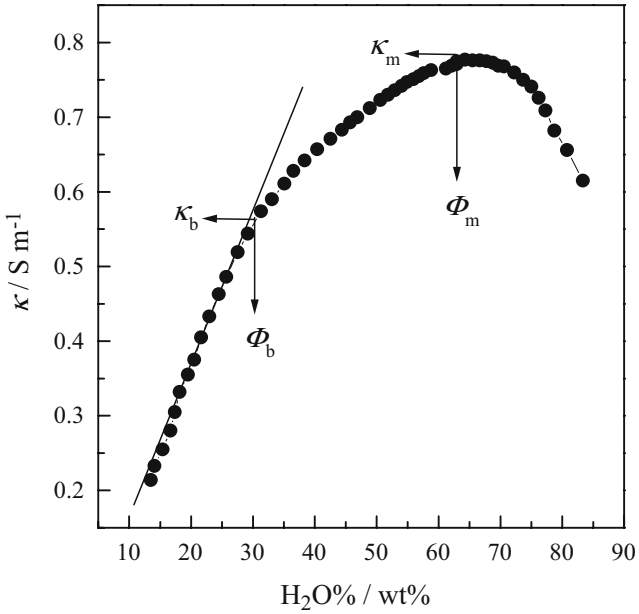

Fig. 6 Conductivity κ as a function of water content in a single-phase microemulsion region. Sample solution was the same as in Fig. 5

used to identify the occurrence of a bicontinuous microemulsion.

The conductivity curve in Fig. 6 clearly illustrates the occurrence of the three microemulsion regions: a water-in-oil region with water content less than 30.3%, an oil-in-water region at water contents greater than 62.4%, and a bicontinuous or oil and water continuous region with water content range from 30.3 to 62.4%.

Conclusions

Mixture of palm-kernel oil with water can be microemulsified to form microemulsions by the use of cetyltrimethylammonium bromide as a surfactant and *iso*-pentanol as a cosurfactant. The size of single-phase microemulsion region is dependent of k_m, *iso*-pentanol-to-CTAB mass ratio. It is found that the maximum microemulsion domain is obtained when k_m is 1.75 under our experimental conditions. The diffusion coefficients of electroactive probe ferrocene in microemulsion medium have been measured by 1.5-order differential electroanalysis. The curve of diffusion coefficient D as a function of the water content reveals to appear three kinds of microstructures of microemulsion. At water contents lower than 29.6%, a water-in-oil microemulsion is formed, and oil is the continuous phase. An oil-in-water region forms at water contents greater than 58.4%. However, a bicontinuous microstructure is observed at water contents in the range 29.6 to 58.4%. The microstructural transition from water-in-oil into oil-in-water by a bicontinuous microemulsion happens completely continuously without any phase separation.

The conductivity curve of microemulsion confirms these results of diffusion measurements. The corresponding values of water content at which microstructural transition occurs are found to be 30.3, 62.4, and 30.3–62.4%, respectively. Thus, the results obtained by the two electrochemical methods, i.e., 1.5-order differential electroanalysis and the conductivity measurements, are in basic agreement. The results reported in this paper show that 1.5-order differential electroanalysis is a useful technique for investigating diffusion properties of microparticles in the organized surfactant solutions. As compared with other electroanalytical methods, the differential electroanalytical technique has the merits of high sensitivity and high resolution. Hence, it can be used at very low electroactive species concentrations and without/or low supporting electrolyte concentrations.

Acknowledgments We acknowledge the Natural Science Foundation (04011432) of Guangdong Province, People's Republic of China for supporting this research. We are also grateful for support from the Grant of the Zhanjiang Normal University.

References

1. Szymula M, Narkiewicz-Michalek J (2006) J Appl Electrochem 36(4):455
2. Yang ZY, Zhao JS, Gao LJ, Wang T, Cao QY, Zhang NY (2006) Anal Lett 39(9):1801
3. Guto M, Rusling JF (2005) J Phys Chem B 109(51):24457
4. Herrero R, Barriada JL, Lopez-Fonseca JM, Moncellim MR, Sastre de Vicente ME (2000) Langmuir 16:5148
5. Mo CS, Zhong MH, Zhong Q (2000) J Electroanal Chem 493:100
6. Miyagishi S (1998) Langmuir 14:7091
7. Santhanalakshmi J, Anandi K (1995) J Colloid Interf Sci 176:226
8. Zana R, Mackay RA (1986) Langmuir 2:109
9. MO CS, Huang ZZ, Zhong MH (1995) Chin Chem Lett 6:415
10. Rusling JF (1994) Electrochemistry in micelles, microemulsions and related organized media. In: Bard AJ (ed) Electroanalytical chemistry, vol 19. Dekker, New York, pp 1–88
11. Gupta S, Mukhopadhyay L, Moulik SP (1995) Indian J Biochem Biophys 32:261
12. Acharya A, Moulik SP, Sanyal SK Mishra BK, Puri PM (2002) J Colloid Interface Sci 245:163
13. Malcolmson C, Barlow DJ, Lawrence MJ (2002) J Pharm Sci 91:2317
14. Navtas TNC, Silva AC, Neto AAD (2001) Fuel 80:75
15. Malcolmson C, Lawrence MJ (1993) J Pharm Pharmacol 45:141
16. Stackelberg MV, Pilgram M, Toome V (1953) Z Electrochem 57:342
17. Lang J, Lalem N, Zana R (1991) J Phys Chem 95:9533
18. Chennamsetty N, Bock H, Scanu LF, Siperstein FR, Gubbins KE (2005) J Chem Phys 122:94710–94711
19. Lopez F, Cinelli G, Ambrosone L, Colafemmina G, Ceglie A, Palazzo G, (2004) Colloids Interf A 237:49
20. Goto M, Ishii D (1975) J Electroanaly Chem 61:361
21. Goto M, Hirano T, Ishii D (1978) Bull Chem Soc Jpn 51:470
22. Ohsawa Y, Aoyagui S (1982) J Electroanal Chem 136:353
23. Gennes PG, Taupin C (1982) J Phys Chem 86:1194
24. Moulik SP, Pal BK (1998) Adv Colloid Interf Sci 78:99
25. Lagourette B, Peyrelasse J, Boned C, Clausse M (1979) Nature 281:61